Materials Research Bulletin 47 (2012) 333–337

Contents lists available at SciVerse ScienceDirect

Materials Research Bulletin

journal homepage: www.elsevier.com/locate/matresbu

# A novel magnetically separable $TiO_2/CoFe_2O_4$ nanofiber with high photocatalytic activity under UV–vis light

Cong-Ju Li [a,*], Jiao-Na Wang [a], Bin Wang [a], Jian Ru Gong [b,*], Zhang Lin [c]

[a] Beijing Key Laboratory of Clothing Materials R&D and Assessment, Beijing Institute of Fashion Technology, Beijing 100029, PR China
[b] National Center for Nanoscience and Technology, China, 11 Zhongguancun Beiyitiao, Beijing 100190, PR China
[c] Fujian Institute of Research on the Structure of Matter, Chinese Academy of Sciences, Fujian 350002, PR China

ARTICLE INFO

*Article history:*
Received 13 January 2011
Received in revised form 10 September 2011
Accepted 8 November 2011
Available online 16 November 2011

*Keywords:*
A. Composites
A. Nanostructures
B. Sol–gel chemistry
C. X-ray diffraction
D. Catalytic properties

ABSTRACT

A novel magnetically separable heterogeneous photocatalyst $TiO_2/CoFe_2O_4$ nanofiber was prepared by sol–gel method and electrospinning technology, followed by heat treatment at 550 °C for 2 h. The phase structure, morphology and magnetic property of the composite nanofibers were characterized by X-ray diffraction, scanning electron microscopy, transmission electron microscope and vibrating sample magnetometer analysis. The photocatalytic studies of $TiO_2/CoFe_2O_4$ fibers suggested that the presence of $CoFe_2O_4$ not only enhanced the absorbance of UV light, but also broadened the response region to visible light. The decolorizing efficiency of methylene blue (MB) solution reaches 95.87% over $TiO_2/CoFe_2O_4$ nanofibers under 300 W Hg lamp after 5 h, which is close to that of Degussa P25. Furthermore, these fibers can be collected with a magnet for reuse and effectively avoid the secondary pollution of the treated water.



## 1. Introduction

In the past three decades, the semiconductor heterogeneous photocatalysis has emerged as an alternative economical and harmless technology for removal of toxic organic pollutants [1,2]. Titanium dioxide ($TiO_2$) is considered as an interesting material and has been widely studied recently because of its optical, electrical and photochemical properties, strong oxidizing power, cost effectiveness and non-toxicity, and it efficiently converts abundant solar energy into effective chemical energy [2–4]. Much progress on the synthesis of nanostructured $TiO_2$ has been made. To enhance its photocatalytic ability, various morphologies of $TiO_2$ including nanoparticles, nanotubes, nanostructured films and nanofibers have been prepared. However, among these nanostructures, nanofibers have a distinctive advantage of being able to form the assembled structures with a high surface area-to-volume ratio and porosity [4,5]. The electrospinning technology has been recognized as an effective, versatile and mature method for the production of nanofibers [6]. This technique was originally invented 70 years ago and has been used primarily for producing ultrathin polymer fibers [7–12].

However, the difficulty of separation and reuse of nanostructured $TiO_2$ from treated water often limits its application in practice. In recent years, some investigators have prepared granular $TiO_2$ with magnetic core and photoactive shell, and proved that the composite nanoparticles could be easily separated by the magnetic field as a result of its magnetic property [13], which can solve an important issue of removing nano-$TiO_2$ from aqueous suspensions. Among the magnetic materials, cobalt ferrite ($CoFe_2O_4$) with the similar crystallization temperature to $TiO_2$ was chosen as a magnetic material in this work. Cubic $CoFe_2O_4$ has been widely studied due to its high electromagnetic performance, excellent chemical stability, mechanical hardness and high cubic magnetocrystalline anisotropy [14].

Based on our previous work [15,16], magnetic inorganic nanofibers have been prepared using electrospinning technology. In order to reclaim $TiO_2$ photocatalysts effectively, we proposed a simple process combined with sol–gel method and electrospinning technology for fabricating magnetic photocatalytic nanofibers of $TiO_2/CoFe_2O_4$, where the spinning aid solution was composed of poly (vinyl pyrrolidone) (PVP), acetic acid and anhydrous alcohol. In the composite nanofiber, the spinel $CoFe_2O_4$ is the magnetic component and $TiO_2$ is the photocatalytic component. In the current experiment, with regard to the $TiO_2/CoFe_2O_4$ fibers, the photocatalytic activity in degradation of methylene blue (MB) under 300 W Hg lamp is close to that of Degussa P25. In addition, the heterogeneous photocatalysts can be separated and collected with a magnet from an aqueous suspension. This is a profound advantage when the catalyst used in practice, because separating ultra-fine catalyst is a serious problem, which impedes the

* Corresponding author.
*E-mail addresses:* congjuli@gmail.com (C.-J. Li), gongjr@nanoctr.cn (J.R. Gong).

0025-5408/$ – see front matter © 2011 Elsevier Ltd. All rights reserved.
doi:10.1016/j.materresbull.2011.11.012

application of $TiO_2$ photocatalysts at industrial scale. Furthermore, this heterogeneous photocatalysts have considerable activity in visible light region and are expect to be used under solar light.

## 2. Experimental

### 2.1. Materials

Cobalt(II) nitrate hexahydrate [$Co(NO_3)_2 \cdot 6H_2O$, 99.0%, A.R. Tientsin Fuchen Chemical Reagents Co.] and iron(III) nitrate ninehydrate [$Fe(NO_3)_3 \cdot 9H_2O$, 98.5%, A.R. Tientsin Yingdaxigui Chemical Reagents Co.] were used as precursors, whereas citric acid monohydrate [$C_6H_8O_7 \cdot H_2O$, 99.5%, Tientsin Yingdaxigui Chemical Reagents Co.] was used as a chelating agent. Ammonia water [$NH_3 \cdot H_2O$, 25%, A.R. Tientsin Yingdaxigui Chemical Reagents Co.] was used to adjust pH of the solution. Poly (vinyl pyrrolidone) [PVP, $M_r$ = 10,000, A.R. Tientsin Damao Chemical Reagents Co.], acetic acid [$CH_3COOH$, A.R. 99.5%, Beijing Chemical Works] and anhydrous alcohol [$CH_3CH_2OH$, A.R. Beijing Chemical Works] were used as a spinning aid. Tetrabutyl titanate ($Ti[O(CH_2)_3CH_3]_4$, A.R. Beijing Xingjin Chemical Plant) was chosen as a Ti resource. Methylene blue (MB, $C_{16}H_{18}ClN_3S \cdot 3H_2O$) was obtained from Beijing Zhongxiyuanda Corporation to act as an organic pollutant in waste water. Degussa P25 (with 80% anatase and 20% rutile) was produced by the Degussa AG Company in Germany.

### 2.2. Preparation of $TiO_2/CoFe_2O_4$ nanofibers

The $CoFe_2O_4$ precursor solution was prepared by dissolving 1.000 g $Co(NO_3)_2 \cdot 6H_2O$, 2.776 g $Fe(NO_3)_3 \cdot 9H_2O$ and 1.980 g $C_6H_8O_7 \cdot H_2O$ in 30.0 ml deionized water. After dissolving the metal precursors, the pH value was regulated to 5–6 with ammonia water. The following evaporation of water at 60 °C resulted in the formation of the precursor gel.

The spinning aid solution was prepared using 4.000 g PVP, 10.0 ml acetic acid and 3.0 ml anhydrous alcohol. Tetrabutyl titanate (1.0 ml) was gradually added into the above solution, and then the mixture was kept stirring at room temperature for about 4–6 h. Eventually, the electrospinning solution was obtained by mixing spinning aid solution with $CoFe_2O_4$ precursor gel (about 3.0 ml) under vigorous stirring for about 12 h.

The prepared electrospinning solution was loaded into a plastic tube (8–9 mm in diameter). The electrospinning process was carried out using our home-made electrospinning system. The spinneret was connected to a positive high-voltage supply (DW-D303-2AC, Tientsin Dongwen High Voltage Power Supply Plant) and the voltage of +18.0 kV was applied. The distance between the spinneret tip and collector was about 14.0 cm. All electrospinning processes were carried out at room temperature. The electrospun fibers were dried at 60 °C for 12 h and calcined at 550 °C for 2 h in air to get $TiO_2/CoFe_2O_4$ fibers at a heating rate of 100 °C/h.

### 2.3. Photocatalytic activity measurement

The photocatalytic activity of the $TiO_2/CoFe_2O_4$ nanofibers was evaluated by the degradation of a model pollutant dye solution, methylene blue (MB), in a photochemical reactor. The bench-scale photochemical reactor system was composed of a cylindrical Pyrex reactor and a light source with vertical irradiation. The light source was a 300 W Hg lamp (with UV light accounting for 40%, Shanghai Bilon Instruments Co., Ltd.) positioned inside a cylindrical Pyrex reactor and surrounded by a circulating water jacket for cooling. 10.0 mg MB was dispersed into 400.0 ml deionized water. Then 25.0 mg $TiO_2/CoFe_2O_4$ fibers were dissolved into above MB solution to form a reaction suspension. Degussa P25 (with 80% anatase and 20% rutile, which was produced by the Degussa AG Company in Germany) was used for comparison. Prior to irradiation, this reaction suspension was magnetically stirred in the dark for 12 h to ensure the establishment of an adsorption/desorption equilibrium of MB on the catalyst surface before illumination. The suspension was irradiated under UV light for 5 h using a 300 W Hg lamp. At a given irradiation time interval (1 h), 3.0 ml aliquots was collected and centrifuged to remove the solid catalyst particles. The absorbance of solution at 663 nm was measured to determine the concentration of MB using an UV–vis spectrophotometer (TU-1901, Beijing Purkinje General Instrument Co., Ltd.) over the wavelength range of 190–800 nm. The equation degradation rate $(D) = [(A_0 - A)/A_0] \times 100\% = [(C_0 - C)/C_0] \times 100\%$ was used to fit experimental data, where $A$ is the absorbance of MB solution after degradation, $A_0$ is the initial absorbance of MB solution before degradation, $C$ is the solution-phase concentration of MB, and $C_0$ is the initial concentration at $t = 0$.

### 2.4. Characterization of $TiO_2/CoFe_2O_4$ nanofibers

The calcined composite nanofibers were characterized by means of X-ray diffraction (XRD) using Cu-Kα radiation with $\lambda = 0.15406$ nm (D/MAX-IIIA, Rigaku, Japan). The morphology of the nanofibers was examined by scanning electron microscopy (SEM, JSM-6360LV, Japan) and transmission electron microscope (TEM, Tecnai $G^2$ 20 S-TWIN). The average diameter of fibers was estimated using image analysis software (JEOL Smile View 2.03) and calculated by selecting a certain amount of fibers randomly observed on the SEM images. The magnetic properties (coercive force $H_c$, specific saturation magnetization $M_s$ and specific remanent magnetization $M_r$) were performed at room temperature by a vibrating sample magnetometer (VSM, Lake Shore 7410) operating up to a maximum field of 20 kG.

## 3. Results and discussion

### 3.1. Crystal structure analysis

The X-ray diffraction pattern for $TiO_2/CoFe_2O_4$ fibers calcined at 550 °C is shown in Fig. 1. All of the main characteristic peaks are indexed as the anatase $TiO_2$ (PDF Card #89-4921), rutile $TiO_2$ (PDF Card #76-0649) and spinel $CoFe_2O_4$ (PDF Card #22-1086) in the standard data. There is a sharp and strong peak of $CoFe_2O_4$ at $2\theta = 35.4°$ and a clear peak of the anatase phase at $2\theta = 25.4°$ in the XRD pattern. However, peaks of impurities ($CoTiO_3$, $FeTiO_3$) at $2\theta = 24.0°$, $32.4°$ and $32.9°$ were observed in the $TiO_2/CoFe_2O_4$ fibers. The average crystallite sizes of anatase $TiO_2$, rutile $TiO_2$ and

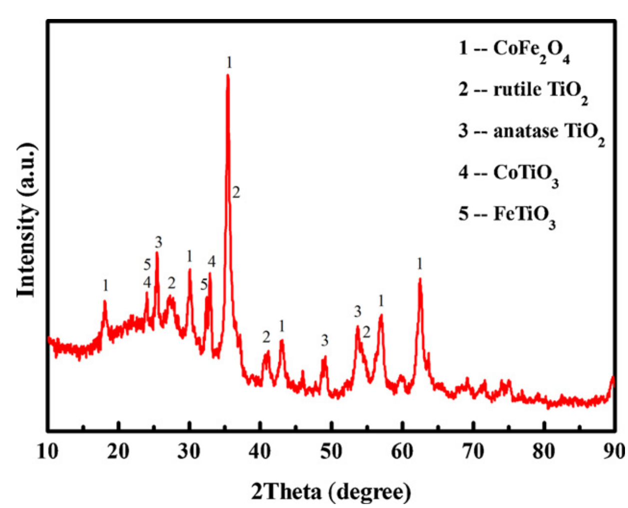


**Fig. 1.** XRD patterns of $TiO_2/CoFe_2O_4$ nanofibers calcined at 550 °C for 2 h.

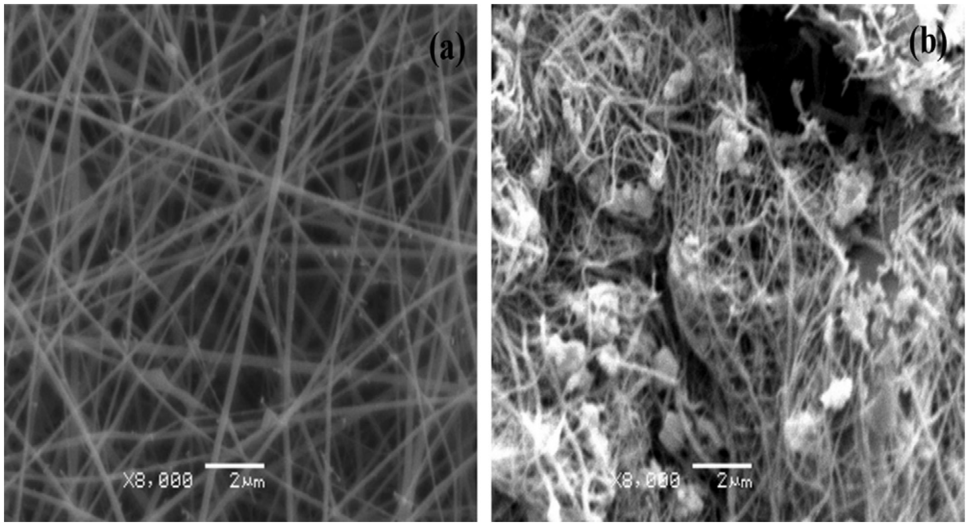


**Fig. 2.** SEM images of $TiO_2/CoFe_2O_4$ nanofibers: (a) as-spun and (b) calcined at 550 °C for 2 h.

spinel $CoFe_2O_4$ were calculated from X-ray line broadening using Scherrer's equation (*i.e.*, $D = 0.89\lambda/(\beta \cos\theta)$, where $\lambda$ is the wavelength of the X-ray radiation, $\theta$ is the diffraction angle and $\beta$ is the full width at half maximum (FWHM)), and were found to be about 20, 15 and 17 nm, respectively. The value of anatase $TiO_2$ was calculated from X-ray line broadening of the reflection peaks of (1 0 1), (2 0 0) and (1 0 5), the value of rutile $TiO_2$ was calculated from the reflection peaks of (1 1 0), (1 0 1), (1 1 1) and (2 1 1), and that of spinel $CoFe_2O_4$ was calculated from the reflection peaks of (1 1 1), (2 2 0), (3 1 1), (4 0 0), (5 1 1) and (4 4 0).

### 3.2. Morphology analysis

Fig. 2(a) and (b) shows the morphology of as-spun and calcined $TiO_2/CoFe_2O_4$ fibers, respectively. As shown in Fig. 2(a), the diameters of the as-spun fibers range from 60 to 240 nm with an average diameter of $130 \pm 34$ nm. The as-spun composite nanofibers appear relatively smooth and uniform due to the amorphous nature of $TiO_2/CoFe_2O_4$/PVP composite [17,18]. As shown in Fig. 2(b), the diameters of the calcined $TiO_2/CoFe_2O_4$ fibers range from 80 to 200 nm with an average diameter of $110 \pm 28$ nm, and the fibers became to shrink with wrinkle because of the decomposition of PVP and the crystallization of $CoFe_2O_4$ and $TiO_2$ [17,18].

The structure of the $TiO_2/CoFe_2O_4$ fiber was observed by TEM in Fig. 3. From Fig. 3(a), a single $TiO_2/CoFe_2O_4$ fiber is demonstrated, which is composed of two kinds of substance with a different contrast, and the surface of the fiber is slightly rough. The high-resolution TEM image of the nanofiber [Fig. 3(b)] reveals that the (3 1 1) and (1 1 1) lattice planes of spinal $CoFe_2O_4$ is of a lattice spacing of 0.24 nm and 0.48 nm respectively. In the standard data of spinel $CoFe_2O_4$ (PDF Card #22-1086), the lattice spacing of (3 1 1) lattice plane is 0.253 nm, and the lattice spacing of (1 1 1) is 0.485 nm. Both of the results are basically consistent. $CoFe_2O_4$ is a magnetic material, and its absorption capacity of electron is much larger than that of $TiO_2$. Thus, the dark part is $CoFe_2O_4$ and the light part is $TiO_2$. The diameter of a single fiber is about 80 nm, which agrees with the result in SEM micrograph [Fig. 2(b)]. Electron diffraction pattern (ED) displays discontinuous diffraction rings [inset of Fig. 3(a)], proving that this composite nanofiber is polycrystalline.

### 3.3. UV–vis diffuse reflectance spectra and photocatalytic activity

To evaluate the photocatalytic activity of $TiO_2/CoFe_2O_4$ fibers, the degradation of MB was investigated. For comparison, the MB degradation over Degussa P25 was also carried out under identical

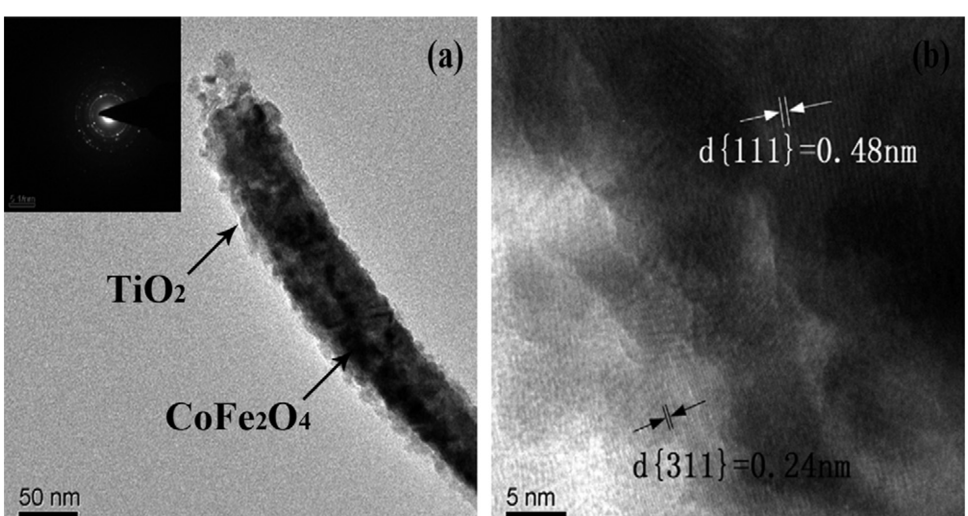


**Fig. 3.** TEM images of $TiO_2/CoFe_2O_4$ nanofibers calcined at 550 °C for 2 h: (a) low-resolution image and (b) high-resolution image.

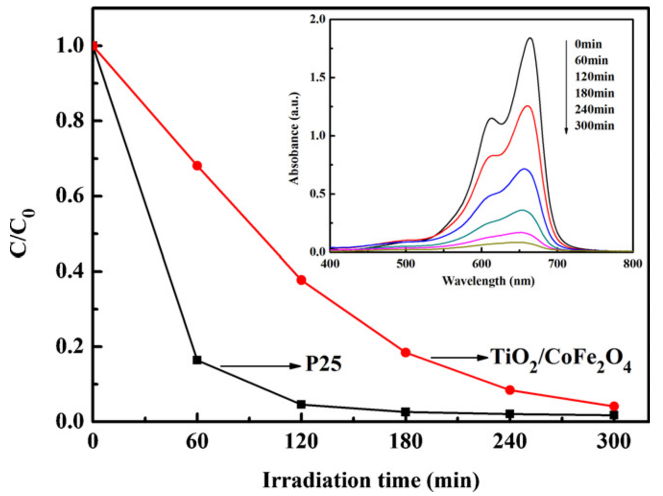


**Fig. 4.** Photocatalytic activity of Degussa P25 and $TiO_2/CoFe_2O_4$ for MB under 300 W Hg lamp irradiation. [Inset figure: UV–vis spectra of MB in aqueous dispersed $TiO_2/CoFe_2O_4$ calcined at 550 °C at different intervals of the irradiation time. Spectra from the top to the bottom refer to irradiation for 0, 1, 2, 3, 4 and 5 h respectively].

conditions. As shown in Fig. 4, the rate of the MB decomposition over Degussa P25, which is known as the best photocatalyst commercially available, is faster than that of $TiO_2/CoFe_2O_4$ fibers in the previous 1 h. However, the photoactivity of $TiO_2/CoFe_2O_4$ (the mass ratio of $TiO_2$ to $CoFe_2O_4$ was 1:3.4) is close to that of pure $TiO_2$ under 5 h of irradiation. Eventually, the decolorizing efficiency of MB solution reaches 95.87% over $TiO_2/CoFe_2O_4$ nanofibers under 300 W Hg lamp after 5 h. This result obviously indicates that the presence of $CoFe_2O_4$ effectively enhances the photocatalytic activity of fiber-like sample. Fig. 5 gives the UV–vis diffuse reflectance spectra of Degussa P25 and $TiO_2/CoFe_2O_4$ composite nanofibers. It can be clearly seen that the intensity of absorbance of composite nanofiber increases significantly in the range of 200–900 nm compared with Degussa P25, which indicates that the band edge absorption has been broadened to visible light region. It is possible that solid solution containing titanium and doping ion (such as $Fe^{3+}$ and $Co^{2+}$) could be formed [19,20] and/or the doping ion could be incorporate into $TiO_2$ lattice by sol–gel method due to the almost same ionic radius of $Fe^{3+}$ (0.64 Å), $Co^{2+}$ (0.65 Å) and $Ti^{4+}$ (0.68 Å). With the substitution for $Ti^{4+}$ by $Fe^{3+}$ or/and $Co^{2+}$ in crystal structure of $TiO_2$, iron–titanium solid solution can introduce a new impurity level to the conduction band of $TiO_2$ and the electrons can be promoted from the valence band to these

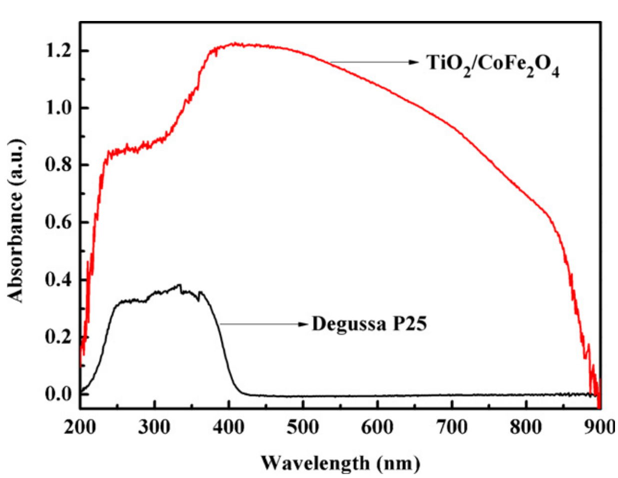


**Fig. 5.** The UV–vis diffuse reflectance spectra of (a) Degussa P25 and (b) $TiO_2/CoFe_2O_4$ nanofibers calcined at 550 °C for 2 h.

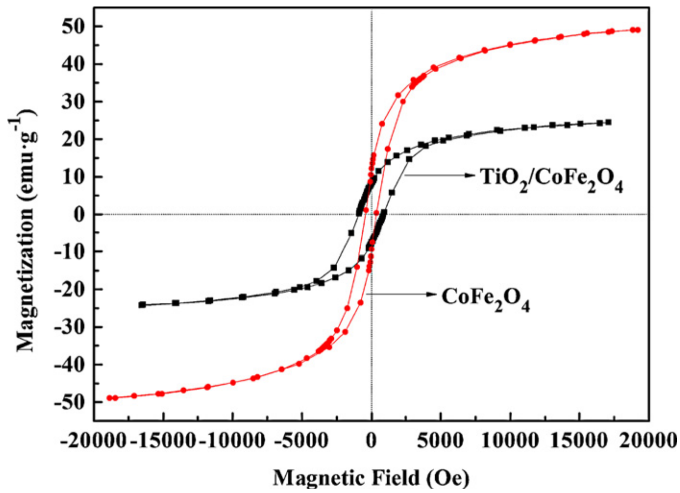


**Fig. 6.** The M-H (magnetization-hysteresis) loops of the $TiO_2/CoFe_2O_4$ and $CoFe_2O_4$ nanofibers calcined at 550 °C for 2 h.

impurity levels [21–23], resulting in a narrowing of bandgap, which is in accordance with the conclusions in other literatures [19,24]. This fact indicates that there are more photogenerated electrons and holes which can be introduced to participate in the photocatalytic reactions. This result is advantageous to broaden the response region of $TiO_2/CoFe_2O_4$ composite nanofibers to visible light and to use solar light as light source in the degradation of dye wastewater.

### *3.4. Magnetic properties and separable ability*

Fig. 6 represents magnetic hysteresis loops of the $TiO_2/CoFe_2O_4$ fibers and pure $CoFe_2O_4$ calcined at 550 °C, measured at room temperature. The values of coercive force ($H_c$), saturation magnetization ($M_s$) and remanent magnetization ($M_r$) are summarised in Table 1. The $M_s$ and $M_r$ values are less than that of pure $CoFe_2O_4$ as a result of the presence of a non-magnetic $TiO_2$ mixing. This result is mainly due to the $M_s$ and $M_r$ values are proportional to the ratio of the magnetic components to the total sample volume [25]. However, the $H_c$ value of $TiO_2/CoFe_2O_4$ fibers (893.71 G) is higher than that of the pure $CoFe_2O_4$ fibers (394.37 G). This indicates that the appearance of $TiO_2$ may be benifit to the permanent magnetic properties.

Coercive force is an important parameter of magnetic materials reflecting the degree of permanent magnetism. It is determined not only by the nature of the material itself, but also by the material microstructures such as grain shape, grain size, degree of irregularity, defects on grain surface, coated condition and so on. In this work, $CoFe_2O_4$ precursor was prepared by sol–gel method. This method makes it fully dissolved and size decreased. And the solution of electrospinning was obtained by mixing PVP/$Ti[O(CH_2)_3CH_3]_4$ solution with cobalt ferrite gel, so the ions were well dispersed with efficient stirring. The presence of $Ti^{4+}$ affected the grain shape and degree of irregularity, and defects on grain surface of $CoFe_2O_4$. All of these issues above are related to the coercive force of $TiO_2/CoFe_2O_4$ composite nanofiber. Moreover, taking into account the low $M_r$ values of $TiO_2/CoFe_2O_4$ fibers, it is

**Table 1**
VSM data for different samples.

| | $H_c$/G | $M_r$/emu g$^{-1}$ | $M_s$/emu g$^{-1}$ |
|---|---|---|---|
| Pure $CoFe_2O_4$ | 394.37 | 11.158 | 49.007 |
| $TiO_2/CoFe_2O_4$ | 893.71 | 10.876 | 33.232 |

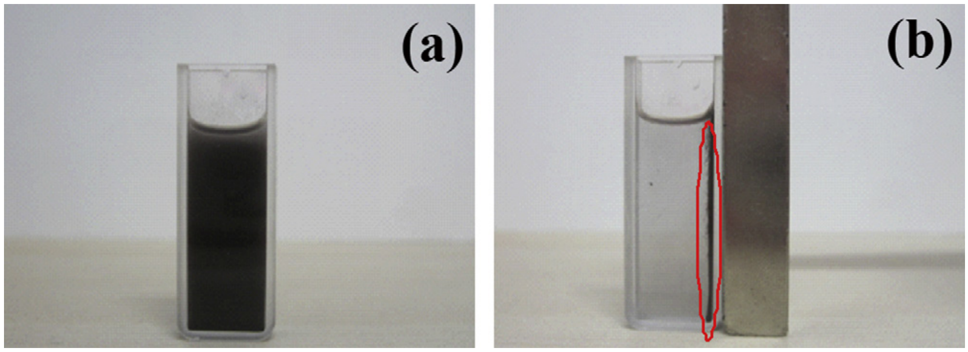


**Fig. 7.** Magnetic photocatalytic nanofibers were separated from treated MB solution.

inferred that the fibers can be redispersed in water after they were separated by an external magnetic field [26].

Finally, the predicted advantage of the composite nanofiber is the association of magnetic and photocatalytic properties in a single fiber. Fig. 7 is a visual evaluation of the magnetic activity, in where $TiO_2/CoFe_2O_4$ heterogeneous photocatalysts suspended in the solution [Fig. 7(a)] and drawn towards the Nd-B magnet [Fig. 7(b)]. The results displayed that the $TiO_2/CoFe_2O_4$ composite nanofibers could be separated and collected with a magnet after photocatalytic reaction.

## 4. Conclusion

In summary, $TiO_2/CoFe_2O_4$ composite nanofibers with an average diameter of $110 \pm 28$ nm were prepared successfully in a straightforward manner by sol–gel method and electrospinning technology. As $Fe^{3+}$ or/and $Co^{2+}$ could substitute $Ti^{4+}$ sites in $TiO_2$ lattice, the presence of $CoFe_2O_4$ not only broadened the response region of visible light but also enhanced the absorbance of UV light. Our work might provide a new insight into the development of novel visible-light-activated photocatalysts. In this experiment, the photocatalytic activity of $TiO_2/CoFe_2O_4$ fibers (the mass ratio of $TiO_2$ to $CoFe_2O_4$ was 1:3.4) is close to that of Degussa P25. Furthermore, these fibers can be separated and collected with a magnet for reuse in photocatalytic process and effectively avoid the secondary pollution of the treated water. This kind of fiber-like photocatalyst has great potential for the practical application in the photocatalytic field.

## Acknowledgements

This study was partly supported by the Natural Science Foundation of China (Grant No. 51073005), the Beijing Natural Science Foundation (Grant Nos. 2112013, KZ201010012012), PHR (IHLB), the 863 Project (Grant No. 2007AA021906), the 973 Project (Grant No. 2010CB933501) and Beijing Municipal Science and Technology Development Program. And also supported by the financial support from Major National Basic Research Development Program (Nos. 2009CB930200 and 2011CB933401), Special Presidential Foundation of Chinese Academy of Sciences (No. O9312911ZX) and National Natural Science Foundations of China (No. Y0191111JJ, 21005023).And also supported by

## References

[1] J. Li, W. Ma, C. Chen, J. Zhao, H. Zhu, X. Gao, J. Mol. Catal. A: Chem. 261 (2007) 131–138.
[2] M.A. Kanjwal, N.A.M. Barakat, F.A. Sheikh, M.S. Khil, H.Y. Kim, Int. J. Appl. Ceram. Technol. 7 (2010) E54–E63.
[3] J.A. Lee, K.C. Krogman, M. Ma, R.M. Hill, P.T. Hammond, G.C. Rutledge, Adv. Mater. 21 (2009) 1252–1256.
[4] S. Xuan, W. Jiang, X. Gong, Y. Hu, Z. Chen, J. Phys. Chem. C 113 (2008) 553–558.
[5] Y.B. Kim, D. Cho, W.H. Park, J. Appl. Polym. Sci. 116 (2010) 449–454.
[6] A.K. Alves, F.A. Berutti, F.J. Clemens, T. Graule, C.P. Bergmann, Mater. Res. Bull. 44 (2009) 312–317.
[7] D. Li, Y. Xia, Adv. Mater. 16 (2004) 1151–1170.
[8] H.R. Darrell, C. Iksoo, Nanotechnology 7 (1996) 216.
[9] A. Frenot, I.S. Chronakis, Curr. Opin. Colloid Interface Sci. 8 (2003) 64–75.
[10] Z.-M. Huang, Y.Z. Zhang, M. Kotaki, S. Ramakrishna, Compos. Sci. Technol. 63 (2003) 2223–2253.
[11] T. Subbiah, G.S. Bhat, R.W. Tock, S. Parameswaran, S.S. Ramkumar, J. Appl. Polym. Sci. 96 (2005) 557–569.
[12] D. Li, J.T. McCann, Y. Xia, M. Marquez, J. Am. Ceram. Soc. 89 (2006) 1861–1869.
[13] Y.S. Chung, S.B. Park, D.-W. Kang, Mater. Chem. Phys. 86 (2004) 375–381.
[14] Z. Zi, Y. Sun, X. Zhu, Z. Yang, J. Dai, W. Song, J. Magn. Magn. Mater. 321 (2009) 1251–1255.
[15] C.-J. Li, J.-N. Wang, Mater. Lett. 64 (2010) 586–588.
[16] L. Cong-ju, X. Guo-rong, Mater. Res. Bull. 46 (2011) 119–123.
[17] Y.-W. Ju, J.-H. Park, H.-R. Jung, S.-J. Cho, W.-J. Lee, Mater. Sci. Eng. B 147 (2008) 7–12.
[18] M. Sangmanee, S. Maensiri, Appl. Phys. A: Mater. Sci. Proc. 97 (2009) 167–177.
[19] J.A. Wang, R. Limas-Ballesteros, T. López, A. Moreno, R. Gómez, O. Novaro, X. Bokhimi, J. Phys. Chem. B 105 (2001) 9692–9698.
[20] J.A. Navío, G. Colón, M. Macías, C. Real, M.I. Litter, Appl. Catal. A: Gen. 177 (1999) 111–120.
[21] X. Yang, C. Cao, L. Erickson, K. Hohn, R. Maghirang, K. Klabunde, Appl. Catal. B: Environ. 91 (2009) 657–662.
[22] J. Zhu, J. Ren, Y. Huo, Z. Bian, H. Li, J. Phys. Chem. C 111 (2007) 18965–18969.
[23] Q. Wang, S. Xu, F. Shen, Appl. Surf. Sci. 257 (2011) 7671–7677.
[24] N.R. Mathews, M.A.C. Jacome, E.R. Morales, J.A.T. Antonio, Phys. Status Solidi (C) 6 (2009) S219–S223.
[25] M. Wan, W. Li, J. Polym. Sci. A: Polym. Chem. 35 (1997) 2129–2136.
[26] Y. Ao, J. Xu, S. Zhang, D. Fu, J. Phys. Chem. Solids 70 (2009) 1042–1047.